Resilience-oriented Transmission Expansion Planning with Optimal Transmission Switching Under Typhoon Weather

Yang Yuan, Heng Zhang, Haozhong Cheng, *Fellow*, *CSEE*, and Zheng Wang

***Abstract*—This paper presents resilience-oriented transmission expansion planning (RTEP) with optimal transmission switching (OTS) model under typhoon weather. The proposed model carefully considers the uncertainty of component vulnerability by constructing a typhoon-related box uncertainty set where component failure rate varies within a range closely related with typhoon intensity. Accordingly, a min-max-min model is developed to enhance transmission network resilience, where the upper level minimizes transmission lines investment, the middle level searches for the probability distribution of failure status leading to max worst-case expected load-shedding (WCEL) under typhoon, and the lower level optimizes WCEL by economic dispatch (ED) and OTS. A nested decomposition algorithm based on benders decomposition is developed to solve the model. Case studies of modified IEEE 30-bus and 261-bus system of a Chinese region illustrate that: a) the proposed RTEP method can enhance resilience of transmission network with less investment than widely used RTEP method based on attacker and defender (DAD) model, b) the influence of OTS on RTEP is closely related with contingency severity and system scale and c) the RTEP model can be efficiently solved even in a large-scale system.**

***Index Terms*—Decomposition algorithm, optimal transmission switching, resilience, transmission expansion planning, uncertainty, vulnerability.**

I. Introduction

In recent years, frequency of extreme weather has been increasing all over the world [1]. Typhoon, ice disaster, earthquake, flood and other extreme weather events often cause serious damage to the power system and bring great challenges to the safe and reliable operation of power systems. In most countries, typhoon prone coastal areas are often economic centers, and the impact of power outage caused by typhoon on these areas is greater than in inland areas. For example, in 2012, super storm Sandy in the United States affected 24 states, resulting in losses of over $60 billion. In 2018, super typhoon Mangkhut caused power failure of nearly 6 million users [2]. Generally, the above extreme weather events are recognized as having high impact and low probability, (HILP) events. The ability of prevention, resistance, absorption and recovery of HILP event is called resilience of power systems [3].

In order to reduce the risk of large-scale blackout under HILP events, it is necessary to improve the resilience of power systems. Power system resilience improvement measures can be divided into long-term measures and short-term measures. Typical long-term measures include transmission/distribution network planning/hardening; risk assessment and management of HILP event, etc. Typical short-term measures include network reconfiguration, optimal line switching, preventive dispatch, generator redispatch, maintenance crew preset load restoration, and so on [4]. Previous research is summarized in the following three parts.

A. Long-term Resilience Improvement Measures

References [5]–[11] improve resilience of system by reducing the vulnerability of components through hardening measures. References [5]–[9] study the optimal hardening strategy of transmission/distribution network, [10] hardens both lines and towers to improve resilience of a distribution network. In particular, [11] has done in-depth research on hardening measures, which utilize four types of hardening measures (the degree of vulnerability improvement and the cost of hardening measures are different) to enhance transmission network resilience under a typhoon disaster. References [12]–[17] improve system resilience through planning measures. [12] proposes a tri-level distribution network planning model against typhoon disaster. [13], [14] make joint planning of transmission network, natural gas or substation to enhance system resilience. Reference [15] proposes a multi-object generation and transmission network expansion planning (GTEP) model against natural disaster, [16] considers microgrids in GTEP, and [17] constructs a tri-level transmission network expansion planning and hardening model against HILP event. It is worth noting [5], [6], [8], [9], [11]–[14], [17] are based on DAD/improved DAD model, of which the advantages and disadvantages are discussed in the research gap part.

B. Short-term Resilience Improvement Measures

References [18]–[23] take network topology optimization

Manuscript received October 20, 2021; revised February 4, 2022; accepted February 21, 2022. Date of online publication October 12, 2022; date of current version March 31, 2023. This work was sponsored by Shanghai Sailing Program under Grant 20YF1418900.

Y. Yuan, H. Zhang (corresponding author, email: zhangheng_sjtu@sjtu.edu.cn; ORCID: https://orcid.org/0000-0002-3710-5573) and H. Z. Cheng are with Key Laboratory of Control of Power Transmission and Conversion, Ministry of Education, Electrical Engineering Department, Shanghai Jiao Tong University, Shanghai, China.

Z. Wang is with State Grid East China Branch, Shanghai, China.

DOI: 10.17775/CSEEJPES.2021.07840

as a short-term resilience improvement measure. In [18]–[20], distribution network reconfiguration is conducted before the typhoon to reduce load-shedding during typhoon. In [21], the location and route of mobile DC de-icing devices are optimized before HILP event. In [22], [23], proactive islanding is adopted to cut off some distribution network lines before snow disaster or flood to form islanding to prevent large-scale cascading failures caused by HILP event. References [24]–[27] improve resilience by optimizing generator scheduling strategy. In [24], [25], proactive dispatching is carried out to reduce output of generators in the area where HILP event might affect, so that unbalanced power caused by the disaster is reduced. In [26], a preventive scheduling strategy consisting of proactive scheduling before disaster and emergency scheduling during disaster are proposed. In [27], a preventive unit commitment model is constructed, which optimizes the day ahead unit commitment and generator redispatch strategy within the day to resist the typhoon disaster.

C. Contingency Modeling Method Under HILP Event

Characterizing uncertainty of contingency under HILP event is the main difficulty in contingency models under HILP events. There are two typical methods. Some studies are based on multi-scenarios method, selecting typical HILP event scenarios and assuming component must outage if the intensity of HILP event reaches the vulnerability threshold [7], [10], [15], [16], [18]–[27], which means component vulnerability is ignored, while others build DAD model, in which high risk components under HILP events are selected according to the vulnerability threshold to form a series of N-k contingency uncertainty sets. The worst-case N-k contingency under HILP event is searched and assumed to occur with 100% probability, ignoring that worst-case contingency only occurs with low probability [5], [6], [8], [9], [11]–[14], [17]. To sum up, both methods only consider the uncertainty of contingency status under HILP event, ignoring the uncertainty of component vulnerability.

D. Research Gap

- Lack of component vulnerability uncertainty modeling method. Vulnerability curve reveals that component vulnerability is closely related with HILP event intensity [3]. There are at least two factors resulting in the uncertainty of component vulnerability. First, the intensity of HILP event is uncertain, and the longer the prediction period, the larger the prediction error. Second, the theoretical vulnerability curve might be different from the actual one, and the longer the component operates, the more significant the difference might be. However, few resilience enhancement models take component vulnerability uncertainty into consideration. Since the uncertainty of HILP event intensity and component vulnerability curve might be more significant in the long term, it is necessary to consider component vulnerability for a resilience enhancement measures model, especially for long-term measures such as TEP and DEP.
- Little research carefully combines TEP and OTS to improve transmission network resilience before and during HILP event. At present, studies combining TEP and OTS can be classified into two kinds: some studies combine DEP and network reconfiguration to improve distribution network resilience [12], [18], while others combine TEP and OTS to improve renewable energy consumption [28]. Few studies combine TEP and OTS to improve resilience of transmission network. Under normal operation conditions, OTS can reduce transmission congestion and delay line investment [29]. However, under HILP events which tend to destroy network topology, whether OTS can take effect on delaying line investment remains to be studied. Moreover, in practice, TEP and OTS are separately decided in planning stage and operation stage, but existing models consider TEP and OTS in a same stage, meaning that OTS is also determined in the planning stage, which is not only unpractical, but also underestimates the effect of OTS during the operation stage.

E. Contributions

Given the above, this paper proposes a RTEP model with OTS to improve resilience of transmission network. The main contributions are as follows:

- Propose a RTEP model considering the vulnerability uncertainty of transmission lines under typhoon weather. To characterize the vulnerability uncertainty, a typhoon-related box uncertainty set of the transmission lines failure rate is constructed, where the actual transmission lines failure rate is assumed to vary with a range closely related with the theoretical failure rate calculated by vulnerability curve under a typical typhoon scenario. Accordingly, the WCEL rather than absolute load-shedding cost is optimized to enhance resilience with less economy cost. To the best known of the author, it is the first time that component vulnerability uncertainty is modeled in a resilience enhancement model. The proposed modeling method can be easily extended to other components and HILP events and the effect of the proposed method is verified by detailed case studies.
- Develop a resilience enhancement model integrating TEP and OTS and evaluate the effect of OTS for RTEP. It is worth mentioning that previous research usually considers OTS and TEP decision variables in the long-term level because they are both binary variables and the transformation of a short-term problem can be facilitated. However, this paper considers TEP and OTS in different levels to make the model more reasonable. TEP as a long-term problem, is optimized as a here-and-now decision variable before HILP events, while OTS as a short-term problem, is decided as a wait-and-see decision variable after HILP events.
- To conquer the computation complexity resulting from consideration of component vulnerability uncertainty and short-term OTS decision in RTEP, a nested decomposition algorithm based on the mindset of benders decomposition is developed to solve the proposed model and efficiency of the algorithm is separately verified in a small and a large system.

The rest of this paper is organized as follows: Section II describes component vulnerability uncertainty modeling method. Section III introduces the mathematical formulation of the proposed TEP model. Section IV describes the solution method. Section V verifies performance of the proposed model on revised IEEE 30-bus and a 261-bus system. Section VI sums up the conclusions.

II. Vulnerability Modeling

In general, the proposed vulnerability model is constructed through three steps. First, a typhoon simulation model is used to generate wind speed on each component. Second, taking wind speed as the input parameter, calculate theoretical failure rate of each component. Third, taking theoretical failure rate as input parameter, form the component vulnerability model. The detailed procedure of each step is presented as follows.

Step 1: Typhoon simulation. Based on Batts typhoon model [30], these formulations are utilized for typhoon.

$$R_{\max} = e^{-0.1239\Delta P^{0.6003}+5.1043}$$

$$V_{gx} = \theta\sqrt{\Delta P} - 0.5R_{\max}f \tag{1}$$

$$V_{R_{\max}} = 0.865V_{gx} + 0.5V_{\mathrm{T}} \tag{2}$$

$$\begin{cases} V_{\mathrm{rin}} = V_{R_{\max}} r/R_{\max} r \le R_{\max} \\ V_{\mathrm{rout}} = V_{R_{\max}} (R_{\max})^x / r r > R_{\max} \end{cases} \tag{3}$$

$$\Delta P = \Delta P_0 - 0.675(1+\sin\phi)t \tag{4}$$

where $R_{\max}$ is the distance from the center of the tropical cyclone to the strongest wind zone, that is, the maximum radius of typhoon. ΔP is the pressure difference (hpa) between the periphery and the center of the tropical cyclone, related to the landing time of the typhoon. V_{gx} is the velocity of air flow caused by pressure gradient force and f the coefficient of Coriolis force of earth rotation. θ is the empirical coefficient and equals to 6.72 in this paper. $V_{R_{\max}}$ is the maximum wind speed, which is reached at $R_{\max}$. V_{T} is the moving speed of typhoon. V_{rin} and V_{rout} are the wind speed when the distance between the element and the typhoon center is less than or greater than $R_{\max}$. r is the distance between the element and the typhoon center. x is a parameter related to the intensity attenuation of typhoon along the radial direction, equals to 0.5∼0.7. ΔP is the central pressure difference; ΔP_0 is the pressure difference between the periphery of the cyclone and the center of the cyclone when the typhoon landed. ϕ is the angle between typhoon track and coastline.

Step 2: Theoretical vulnerability calculation. The vulnerability model proposed by [31] is used. This model indicates the component failure rate during typhoon will evidently increase only if wind speed exceeds the wind speed threshold, which has been proofed in the Northeast U.S. power system. The failure rate of transmission line at time t in a typhoon disaster can be calculated as:

$$\lambda_t^l(w_t) = \begin{cases} \left[1+\kappa\left(\frac{w_t^2}{w_r^2}-1\right)\right]\lambda_{\mathrm{norm}}, & \text{if } w_t > w_r \\ \lambda_{\mathrm{norm}}, & \text{if } w_t \le w_r \end{cases} \tag{5}$$

where w_t is the wind speed at time t. w_r is the wind speed threshold. κ is the sensitive factor of failure rate to wind speed. λ_{norm} is the normal failure rate without typhoon.

Step 3: Transmission lines vulnerability modeling. This paper assumes the actual failure rate of transmission lines fluctuates near the theoretical failure rate derived from (5), and the failure rate and failure state of transmission lines under typhoons are expressed as follows. It worth mentioning this paper focuses on transmission lines which are generally more vulnerable than other transmission system components, such as tower, substation, and so on [8], however, this vulnerability model can be easily extended to those components by merely changing the failure rate interval.

$$\begin{aligned} \mathcal{D} := \{ & P \in \mathcal{M}_+(\Omega) : \underline{\lambda}_t^l \le \mathrm{E}_p[1-z_{lt}] \le \overline{\lambda}_t^l, t \in T \\ & \overline{\lambda}_t^l = k_1\lambda_t^l, k_1 > 1 \\ & \underline{\lambda}_t^l = k_2\lambda_t^l, 0 < k_2 < 1\} \end{aligned} \tag{6}$$

$$\Omega := \left\{ z_{lt} \in \{0,1\} : \sum_{l\in L} z_{lt} \ge N_L - K_{\max}, t \in T \right\} \tag{7}$$

where $\mathcal{D}$ is the ambiguity set composed of failure status probability distribution of transmission lines. $\mathcal{M}_+$ is the support set of transmission lines failure status, that is, a set composed of probability distribution of transmission lines failure status P. Set Ω means the number of lines which outage time t should be less than $K_{\max}$. $z_{lt} = 1$ indicates that line l is normal at time t, $z_{lt} = 0$ indicates that line l is out of service at time t. L is the set of all transmission lines. $\mathrm{E}_p[1-z_{lt}]$ is the expected value of the failure state of line l at time t, that is, the actual failure rate of line l at time t. λ_t^l is the theoretical failure rate of t line l at time, which is derived from (5). $\overline{\lambda}_t^l$ and $\underline{\lambda}_t^l$ are the upper and lower limits of the actual failure rate of line l at time t. It worth mentioning that in practice, $\overline{\lambda}_t^l$ and $\underline{\lambda}_t^l$ can be obtained by setting a specific range of typhoon category or setting different realistic vulnerability curves. After each occurrence of typhoon, new line failure rate data (although limited) can be used to adjust the range if it is too small or too large, which means the proposed vulnerability model can learn from historical data and better prepare for next extreme event. Moreover, the proposed vulnerability model can be easily extended to other components (e.g. generators, substations) and other HILP events.

III. Problem Formulation

A. Model Overview

Resourcefulness, robustness, adaptivity and rapid recovery are four main features of a resilient power system, and these features can be reflected in system performance in face of a HILP event, as shown in Fig. 1 [3]. Phase 1 is preparedness before a HILP event, and preventive measures can be taken to enhance resourcefulness of system. Phase 2 is resistance during a HILP event, corrective measures can be taken to maintain the performance of system at an acceptable level, that is, to enhance robustness of system. Phase 3 is response at post-event degraded state, during which restoration measures can be taken to start phase 4. Phase 4 is recovery. It worth mentioning the proposed RTEP model focuses on preparedness and resistance phase and ignores the recovery phase, utilizing

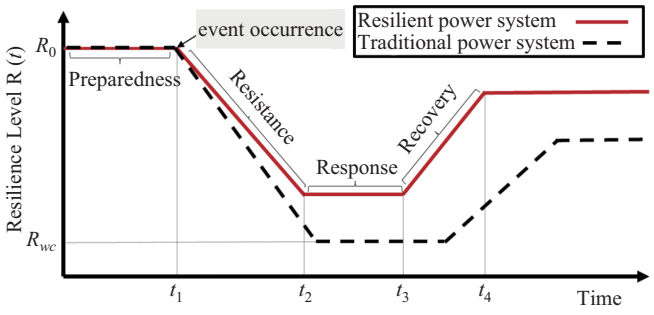

Fig. 1. The performance of resilient power system under HILP event.

TEP and OTS as preventive and corrective measures to enhance resourcefulness and robustness of a power system.

The framework of the proposed RTEP with OTS model is presented in Fig. 2. The model is a two-stage tri-level optimization problem. The first stage deals with long-term problems, including the first level problem which minimizes investment of transmission lines. The second stage deals with short-term problems and includes level 2 and level 3 problems, which searches for the probability distribution of failure status causing max WCEL under a typhoon and minimizes the WCEL by ED and OTS. The vulnerability modeling procedure is carried out and embedded into the level 2 problem. Considering that for an HILP event, high impact is related to not only the loss but also the probability of the loss. This paper employs WCEL rather than the worst-case load-shedding (WCL) used in DAD based RTEP model to consider the loss and its probability during an extreme event, which can better tradeoff the conservativeness and economy of the RTEP model.

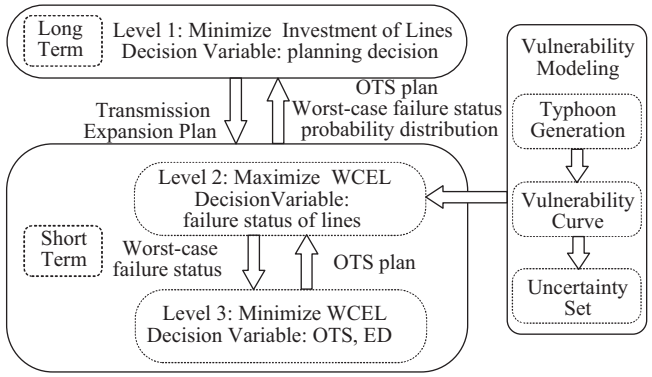

Fig. 2. The framework of the proposed RTEP with OTS model.

B. Model Formulation

The mathematical formulation of the proposed RTEP with OTS model is described as follows.

$$\min_{\boldsymbol{x},v}\left\{\sum_{l\in L_c} C_l x_l + \sup_{P\in\mathcal{D}} \mathrm{E}_p[f(\boldsymbol{x},\boldsymbol{z})]\right\} \tag{8}$$

subject to

$$\sum_{l\in L_c} C_l x_l \le \prod_{L} \tag{9}$$

$$x_l \in \{0,1\} \tag{10}$$

where x_l is investment decision variable of line l, $x_l = 1$ represents line l is built, otherwise $x_l = 0$, and C_l is its investment cost of line l, L_c is the set of candidate lines. $\mathrm{E}_p[f(x,z)]$ represents expected load-shedding cost caused by typhoon and $\sup_{P\in\mathcal{D}} \mathrm{E}_p[f(x,z)]$ searches for typhoon-related failure status probability distribution P in ambiguity set $\mathcal{D}$ which results in max $\mathrm{E}_p[f(x,z)]$. Therefore, the vulnerability uncertainty model introduced in part II is integrated into the second level of RTEP model. $f(x,z)$ represents minimum load-shedding cost for a given transmission line decision x_l and the worst-case failure status probability distribution P, and $f(x,z)$ equals to the following problem.

$$\min_{v,\Delta D_{bt}} \sum_{t\in T}\sum_{b\in B} C_b \Delta D_{bt} \tag{11}$$

$$\sum_{g\in G} p_{gt} + \sum_{l\in L^+(b)} p_{lt} - \sum_{l\in L^-(b)} p_{lt} = \sum_{b\in B}(D_{bt} - \Delta D_{bt}),$$
$$\forall t\in T, \forall b\in B \tag{12}$$

$$-(2 - z_{lt} - v_l)M \le p_{lt} - B_l(\theta_{s(l)t} - \theta_{e(l)t}),$$
$$\forall t\in T, \forall l\in L_e$$

$$p_{lt} - B_l(\theta_{s(l)t} - \theta_{e(l)t}) \le (2 - z_{lt} - v_l)M,$$
$$\forall t\in T, \forall l\in L_e \tag{13}$$

$$-z_{lt}p_l \le p_{lt} \le z_{lt}\bar{p}_l, \forall t\in T, \forall l\in L_e$$

$$-v_l p_l \le p_{lt} \le v_l \bar{p}_l, \forall t\in T, \forall l\in L_e \tag{14}$$

$$-(1 - x_l)M \le p_{lt} - B_l(\theta_{s(l)t} - \theta_{e(l)t}), \forall t\in T, \forall l\in L_c$$

$$p_{lt} - B_l(\theta_{s(l)t} - \theta_{e(l)t}) \le (1 - x_l)M, \forall t\in T, \forall l\in L_c \tag{15}$$

$$-x_{lt}p_l \le p_{lt} \le x_{lt}\bar{p}_l, \forall t\in T, \forall l\in L_c \tag{16}$$

$$0 \le p_{gt} \le p_{g\max}, \forall t\in T, \forall g\in G \tag{17}$$

$$0 \le \Delta D_{bt} \le D_{bt}, \forall t\in T, \forall b\in B \tag{18}$$

$$\sum_{l\in L_e}(1 - v_l) \le N_{\mathrm{v}}, \forall l\in L_e \tag{19}$$

$$\underline{\theta}_b \le \theta_{bt} \le \bar{\theta}_b, \forall t\in T, \forall b\in B \tag{20}$$

Constraint (12) represents the power balance equation, where p_{gt} is output of generator g at time t, G is the set of generators, p_{lt} is power flow in line l at time t, $L^+(b)$ is the set of lines on which the power flows into bus b, $L^-(b)$ is the set of lines on which the power flows out of bus b.D_{bt} is the load demand at bus b at time t, ΔD_{bt} is the load-shedding at bus b at time t, and B is the set of buses. (13) and (15) represents power flow of existing lines and candidate lines respectively, where v_l is the transmission lines switching decision variable, $v_l = 0$ line l is switched off during typhoon, otherwise $v_l = 1$. L_c is the set of existing lines. (14) and (16) limits power flow of existing lines and candidate lines, respectively. (17) limits the output of each generator, (18) limits the load shedding at each node, (19) limits the amount of switchable lines, (20) limits the phase angles.

IV. Solution Method

A nested decomposition algorithm based on benders decomposition is developed to solve the proposed model. First, we rewrite the model in a compact form:

$$\min_{\boldsymbol{x}} \left\{ \boldsymbol{c}_l^{\mathrm{T}} \boldsymbol{x} + \sup_{P \in \mathcal{D}} \mathrm{E}_p[f(\boldsymbol{x}, \boldsymbol{z})] \right\} \tag{21}$$

subject to

$$\boldsymbol{A}\boldsymbol{x} \le \boldsymbol{b},\ \boldsymbol{x} \in \{0,1\}^{|L_c|} \tag{22}$$

where $f(\boldsymbol{x}, \boldsymbol{z})$ can be represented as follows:

$$\min_{\boldsymbol{y}} \boldsymbol{c}_d^{\mathrm{T}} \boldsymbol{y} \tag{23}$$

$$\text{s.t.}\quad \boldsymbol{B}\boldsymbol{y} + \boldsymbol{C}\boldsymbol{v} + \boldsymbol{D}(\boldsymbol{z}) \ge \boldsymbol{d} \tag{24}$$

$$\boldsymbol{E}\boldsymbol{y} + \boldsymbol{F}(\boldsymbol{x}) \ge \boldsymbol{f} \tag{25}$$

$$\boldsymbol{G}\boldsymbol{y} \ge \boldsymbol{g} \tag{26}$$

$$\boldsymbol{H}\boldsymbol{v} \ge \boldsymbol{h} \tag{27}$$

where $\boldsymbol{x}$, $\boldsymbol{y}$ and $\boldsymbol{v}$ represent the first stage decision vector, the second stage continuous decision vector and the second stage binary decision vector. (22) represents (9)–(10), (24) represents (13)–(14), (25) represents (15)–(16), (26) represents (12), (17)–(18), (20), and (27) represents (19).

We rewrite $\underline{\lambda}_t^l \le \mathrm{E}_p[1 - z_{lt}] \le \overline{\lambda}_t^l, t \in T$ as $\mathrm{E}_p[\boldsymbol{Y}\hat{\boldsymbol{z}}] \le \hat{\boldsymbol{\lambda}}$, where $\hat{\boldsymbol{z}} = \boldsymbol{I} - \boldsymbol{z}$, $\hat{\boldsymbol{\lambda}} = [\overline{\boldsymbol{\lambda}}^{\mathrm{T}}, \underline{\boldsymbol{\lambda}}^{\mathrm{T}}]^{\mathrm{T}}$, and $\boldsymbol{Y} = [\boldsymbol{I}, -\boldsymbol{I}]^{\mathrm{T}} \in \mathrm{R}^{2|L_e| \times |L_e|}$. Then, rewrite $\sup_{P \in \mathcal{D}} \mathrm{E}_p[f(\boldsymbol{x}, \boldsymbol{z})]$ as follows.

$$\sup_{P \in \mathcal{D}} \mathrm{E}_p[f(\boldsymbol{x}, \boldsymbol{z})] = \max\nolimits_{P(\boldsymbol{z})} \sum_{\boldsymbol{z} \in \Omega} f(\boldsymbol{x}, \boldsymbol{z}) P(\boldsymbol{z}) \tag{28}$$

$$\text{s.t.}\quad \sum_{\forall \boldsymbol{z} \in \Omega} \boldsymbol{Y}\hat{\boldsymbol{z}} P(\boldsymbol{z}) \le \hat{\boldsymbol{\lambda}} \tag{29}$$

$$\sum_{\forall \boldsymbol{z} \in \Omega} P(\boldsymbol{z}) = 1 \tag{30}$$

where (28)–(30) represent that this problem searches for the worst-case probability of the contingency $P(\boldsymbol{z})$ within the ambiguity set $\mathcal{D}$ for any possible contingency status $\boldsymbol{z} \in \Omega$. In light of strong dual theory, (28)–(30) equals the following problem.

$$\min_{\tau \ge 0, \alpha} \hat{\boldsymbol{\lambda}}^{\mathrm{T}} \tau + \alpha \tag{31}$$

$$\text{s.t.}\quad \boldsymbol{\tau}^{\mathrm{T}} \boldsymbol{Y}\hat{\boldsymbol{z}} + \alpha \ge f(\boldsymbol{x}, \boldsymbol{z}),\ \forall \boldsymbol{z} \in \Omega \tag{32}$$

where τ and α are the dual variables of (29) and (30). Thus, problem (21) can be described as:

$$\text{(P1)}\quad \min_{\boldsymbol{x}, \tau \ge 0, \alpha} \boldsymbol{c}_l^{\mathrm{T}} \boldsymbol{x} + \hat{\boldsymbol{\lambda}}^{\mathrm{T}} \tau + \alpha \tag{33}$$

$$\text{s.t.}\quad \alpha \ge f(\boldsymbol{x}, \boldsymbol{z}) - \boldsymbol{\tau}^{\mathrm{T}} \boldsymbol{Y}\hat{\boldsymbol{z}},\ \forall \boldsymbol{z} \in \Omega \tag{34}$$

$$(22) \tag{35}$$

Since (34) contains contingency scenarios with exponential growth as $K_{\max}$ increases, (36) are introduced to replace (34).

$$\text{s.t.}\quad \alpha \ge \max\nolimits_{\boldsymbol{z} \in \Omega} \left\{ f(\boldsymbol{x}, \boldsymbol{z}) - \boldsymbol{\tau}^{\mathrm{T}} \boldsymbol{Y}\hat{\boldsymbol{z}} \right\} \tag{36}$$

Based on (33), (35), (36), the solution algorithm utilizing benders decomposition is described as follows.

A. Sub-problem (SP)

At each iteration m, for a given $\boldsymbol{x}^{(m)}$, sub-problem searches for the corresponding worst-case contingency probability distribution $P(\boldsymbol{z}) \in \mathcal{D}$ that results in the maximum expected load-shedding. The process is completed by solving $\max_{\boldsymbol{z} \in \Omega} \{ f(\boldsymbol{x}, \boldsymbol{z}) - \boldsymbol{\tau}^{\mathrm{T}} \boldsymbol{Y}\hat{\boldsymbol{z}} \}$, which is bilevel programming.

Strong dual theory are often utilized to transform (36) to a single level maximum problem, however, in the proposed model, $f(\boldsymbol{x}, \boldsymbol{z})$ contains binary decision variable $\boldsymbol{v}$, disabling the direct use of strong dual theory. Therefore, the following iterative algorithm is designed to solve $\max_{\boldsymbol{z} \in \Omega} \{ f(\boldsymbol{x}, \boldsymbol{z}) - \boldsymbol{\tau}^{\mathrm{T}} \boldsymbol{Y}\hat{\boldsymbol{z}} \}$.

Step 1: set lower bound $LB_{\mathrm{SP}} := -\infty$ and upper bound $UB_{\mathrm{SP}} := +\infty$, for inner iteration j, initialize $\boldsymbol{v} = \boldsymbol{v}^{(j)}$.

Step 2: for given $\boldsymbol{x}^{(m)}$, $\boldsymbol{\tau}^{(m)}$ and $\boldsymbol{v}^{(j)}$, $f(\boldsymbol{x}, \boldsymbol{z})$ turns into a linear programming (LP) problem, thus strong dual theory can be used to merge $\max_{\boldsymbol{z} \in \Omega} \left\{ f(\boldsymbol{x}, \boldsymbol{z}) - \boldsymbol{\tau}^{\mathrm{T}} \boldsymbol{Y}\hat{\boldsymbol{z}} \right\}$ into one level maximum problem SP1 as follows.

$$\max_{\boldsymbol{\beta}, \boldsymbol{\eta}, \boldsymbol{\delta}} \Big\{ \left(\boldsymbol{d} - \boldsymbol{C}\boldsymbol{v}^{(j)} - \boldsymbol{D}(\boldsymbol{z}) \right)^{\mathrm{T}} \boldsymbol{\beta} + \left(\boldsymbol{f} - \boldsymbol{F}\left(\boldsymbol{x}^{(m)} \right) \right)^{\mathrm{T}} \boldsymbol{\eta} + \boldsymbol{g}^{\mathrm{T}} \boldsymbol{\delta} - \boldsymbol{\tau}^{(m)\mathrm{T}} \boldsymbol{Y}\hat{\boldsymbol{z}} \Big\} \tag{37}$$

$$\text{s.t.}\quad \boldsymbol{B}^{\mathrm{T}} \boldsymbol{\beta} + \boldsymbol{E}^{\mathrm{T}} \boldsymbol{\eta} + \boldsymbol{G}^{\mathrm{T}} \boldsymbol{\delta} \le \boldsymbol{c_d} \tag{38}$$

$$\boldsymbol{\beta}, \boldsymbol{\eta}, \boldsymbol{\delta} \ge 0 \tag{39}$$

$$\boldsymbol{K}\boldsymbol{z} \ge \boldsymbol{l_k} \tag{40}$$

where $\boldsymbol{\beta}, \boldsymbol{\eta}, \boldsymbol{\delta}$ represent the dual vector of (24)–(26), (40) represents (7). Record the solution and optimal objective function value of SP1 as $\boldsymbol{z}^{(j)}$ and $V_{\mathrm{SP1}}^{(j)}$, update $UB_{\mathrm{SP}} = V_{\mathrm{SP1}}^{(j)}$.

Step 3: for given $\boldsymbol{x}^{(m)}$ and $\boldsymbol{z}^{(j)}$, solve minimum problem $f\left(\boldsymbol{x}^{(m)}, \boldsymbol{z}^{(j)} \right)$, denoted as SP2, record the solution and optimal objective function value of SP2 as $\boldsymbol{v}^{(j+1)}$ and $V_{\mathrm{SP2}}^{(j)}$, update $LB_{\mathrm{SP}} = V_{\mathrm{SP2}}^{(j)}$.

Step 4: If $(UB_{\mathrm{SP}} - LB_{\mathrm{SP}})/LB_{\mathrm{SP}} \le \upsilon$, inner iteration stops, record $\boldsymbol{v}^{(m)} = \boldsymbol{v}^{(j+1)}$, $\boldsymbol{z}^{(m)} = \boldsymbol{z}^{(j)}$, $\boldsymbol{\beta}^{(m)} = \boldsymbol{\beta}^{(j)}$, $\boldsymbol{\eta}^{(m)} = \boldsymbol{\eta}^{(j)}$, $\boldsymbol{\delta}^{(m)} = \boldsymbol{\delta}^{(j)}$, and set $UB = LB_{\mathrm{SP}} - \alpha^{(m)} + V_{\mathrm{MP}}^{(m)}$ for P1 and go to master problem (MP) of outer iteration. If not, $j = j + 1$ and go to step 2.

B. Master Problem

At m iteration, for given $\boldsymbol{v}^{(m)}$ and $\boldsymbol{z}^{(m)}$, the MP can be expressed as follows.

$$\min_{\boldsymbol{x}, \tau \ge 0, \alpha} \boldsymbol{c}_l^{\mathrm{T}} \boldsymbol{x} + \hat{\boldsymbol{\lambda}}^{\mathrm{T}} \tau + \alpha \tag{41}$$

$$(22) \tag{42}$$

$$\alpha \ge \left(\boldsymbol{d} - \boldsymbol{C}\boldsymbol{v}^{(m)} - \boldsymbol{D}\left(\boldsymbol{z}^{(m)} \right) \right)^{\mathrm{T}} \boldsymbol{\beta}^{(m)} + \left(\boldsymbol{f} - \boldsymbol{F}(\boldsymbol{x}) \right)^{\mathrm{T}} \boldsymbol{\eta}^{(m)} + \boldsymbol{g}^{\mathrm{T}} \boldsymbol{\delta}^{(m)} - \boldsymbol{\tau}^{\mathrm{T}} \boldsymbol{Y}\hat{\boldsymbol{z}}^{(m)} \tag{43}$$

where (43) is cut generated by dual variables obtained from (SP). Record the solution and objective function value of MP as $\boldsymbol{x}^{(m+1)}, \alpha^{(m+1)}, \tau^{(m+1)}$ and $V_{\mathrm{MP}}^{(m+1)}$, then set $LB = V_{\mathrm{MP}}^{(m+1)}$ for P1. If $(UB - LB)/LB \le \upsilon$, the outer iteration stops and $\boldsymbol{x}^{(m+1)}$ is the final transmission expansion plan, otherwise $m = m + 1$ and go to SP. The flowchart of the proposed nested algorithm is presented in Fig. 3.

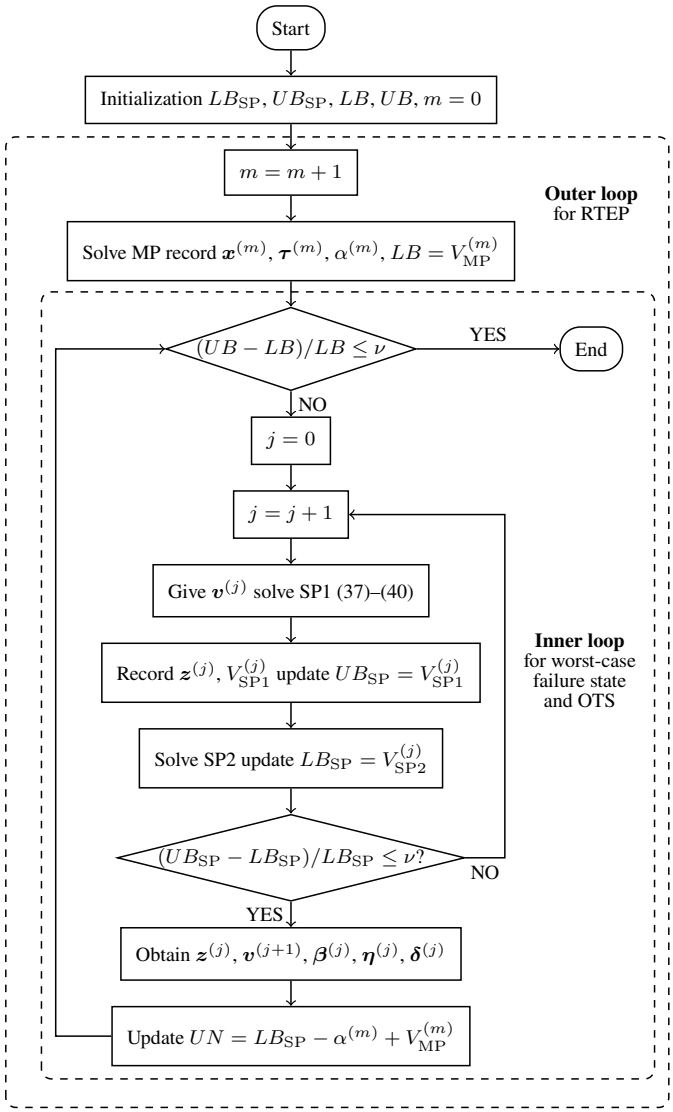

Fig. 3. Flowchart of the proposed nested algorithm.

V. Case Study

A. Modified IEEE 30-bus System

Modified IEEE 30-bus system (shown as Fig. 4) consists of 8 generators and 41 transmission lines and 41 candidate lines, which are numbered in Fig. 4. This system is assumed to be located in an area of 40000 square kilometers. The initial max wind speed and the moving speed are separately set to be 40 m/s and 12 km/h, and the angle between typhoon moving track and horizontal axis is 45°. According to (1)–(4), the typhoon is simulated and presented every 2 h in Fig. 4. For vulnerability model, w_r and κ are set to 20 m/s and 0.7 [7], while k_1 and k_2 are set to 1.15 and 0.85, that is, the max deviation between actual and predicted failure rate of component is ±15%. Load shedding cost is set to be 10 M$/p.u. Investment cost of the line is proportional to its reactance and is approximately 1 M$/year, other system parameters are given in MATPOWER. The program is developed with Matlab R2016a on a PC with Intel(R) core (TM) i5-7200U. In this part, we conduct case studies to analyze TEP, OTS and resilience index (WCEL) results under three typical uncertain factors related with typhoon weather: 1) contingency severity, 2) frequency of typhoons in one year which is reflected by cost of load-shedding (CL), and 3) wind speed prediction error during typhoon weather which is reflected by vulnerability uncertainty (VU).

B. Effectiveness of the Proposed RTEP Model

Two cases are designed to demonstrate the advantages of RTEP model, shown in Tables I and II.

Case 1 (C1): the proposed RTEP model with different contingency severity (N-0∼N-6) for IEEE 30-bus system, and OTS is ignored in C1.

Case 2 (C2): the DAD model with different contingency severity (N-2∼N-6) for IEEE 30-bus system. The difference between DAD model and RTEP is the uncertain contingency set of DAD model only includes (7).

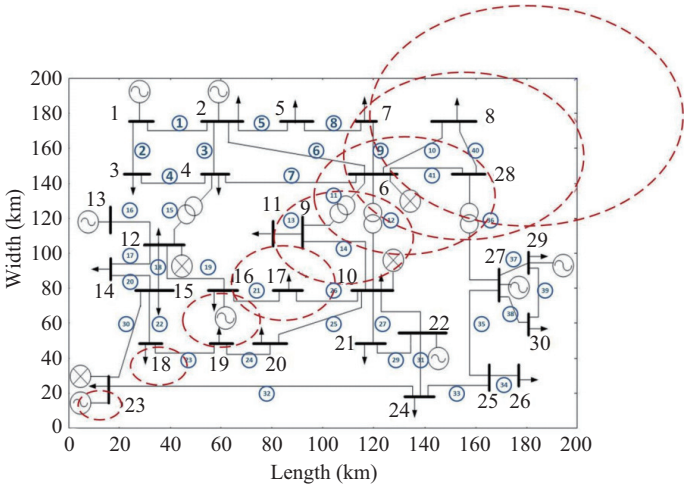

Fig. 4. The modified IEEE 30-bus test system and simulated typhoon.

TABLE I
Results of RTEP with Different Contingency Severity

C1	IC (M$)	LC (M$)	WCEL (MW)	EP	NEL
N-0	0	0	0	–	0
N-1	1.98	0	0	9, 29	2
N-2	3.05	0.71	7.08	9, 10, 29	3
N-3	3.05	0.92	9.22	9, 10, 29	3
N-4	9.49	1.36	13.62	9, 10, 15, 18, 24, 25, 26, 29, 37	9
N-5	12.6	2.01	20.1	9, 10, 15, 16, 18, 24, 25, 26, 29, 35, 36, 37	12
N-6	16.64	2.53	25.31	7, 9, 10, 11, 14, 15, 16, 18, 24, 25, 26, 27, 29, 35, 36, 37	16

TABLE II
Results of RTEP and DAD with Different Contingency Severity

	C1			C2		
	IC (M$)	LC (M$)	WCEL (MW)	IC (M$)	LC (M$)	WCEL (MW)
N-2	3.05	0.81	8.13	4.21	1.261	12.61
N-3	3.05	0.92	9.22	6.23	1.404	14.04
N-4	9.49	1.36	13.62	11.74	2.047	20.47
N-5	12.6	2.01	20.1	16.01	2.59	25.9
N-6	16.64	2.53	25.31	18.82	3.135	31.35

It can be seen that from N-2∼N-6, the investment cost (IC) and the load-shedding cost (LC) of both C1 and C2 increase. However, from N-2∼N-6, the IC and LC of RTEP keep less than of DAD model, which proofs the proposed RTEP model can obtain a less conservative expansion plan (EP) than DAD model without sacrificing resilience, that is, the RTEP has better tradeoff resilience and economy cost than DAD model. Moreover, the number of expansion lines (NEL) remains 3 from N-2∼N-3 in C1, representing that in this case, building transmission lines 9, 10, 29 is enough to resist typhoon disaster at the least economy cost.

C. Resilience Enhancement Effect of the RTEP Model

To illustrate the resilience enhancement effect of RTEP and OTS, case studies are carried out by comparing results of traditional TEP (TTEP) and RTEP with different number of switchable lines (NSL), NSL = 0, 3, 6 and switched off lines (SOL) as shown in Table III, Figs. 5 and 6. Moreover, the load percentage (LP) defined by (44) during the simulated typhoon disaster with different NSL and TEP model under N-2 contingency are presented in Fig. 7.

$$LP(t) = \frac{\sum_{b\in B}(D_{bt} - \Delta D_{bt})}{\sum_{b\in B} D_{bt}},\ \forall t \in T \qquad (44)$$

TABLE III
RESULTS OF RTEP WITH DIFFERENT NSL

N-2	IC (M$)	LC (M$)	WCEL (MW)	EP	SOL
TTEP	0	1.04	10.43	–	0
NSL = 0	3.05	0.71	7.08	9, 10, 29	0
NSL = 3	2.07	0.69	5.95	9, 10	30, 40, 41
NSL = 6	2.07	0.52	5.17	9, 10	1, 6, 14, 40, 41
N-4	IC (M$)	LC (M$)	WCEL (MW)	EP	SOL
NSL = 0	9.49	1.36	13.62	9, 10, 15, 18, 24, 25, 26, 29, 37	0
NSL = 3	8.47	1.25	12.48	9, 10, 15, 24, 25, 26, 29, 37	3, 30, 41

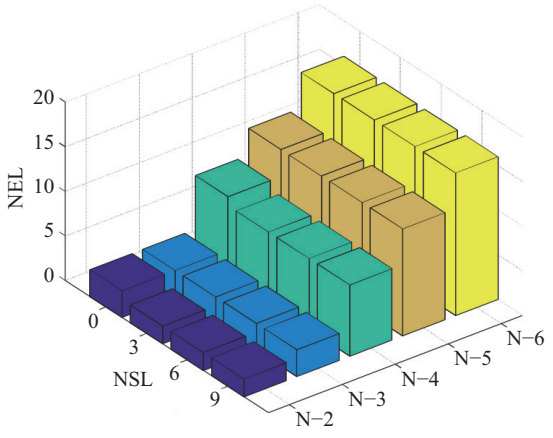

Fig. 5. NEL results with different NSL and different contingency severity.

From the figure and table above, the following conclusions can be drawn.

1) Both RTEP and OTS can enhance power system resilience by improving resourcefulness and robustness of a system, and the resilience enhancement effect of RTEP is more evident than of OTS. Compared with TTEP, load-shedding of RTEP during the typhoon with 0, 3, 6 NSL are only 68%, 57%, 50% of TTEP.

2) OTS takes effect on resistance against typhoon weather mainly by actively switching off transmission lines which are relatively more vulnerable in typhoon weather, but locate in an area where transmission lines are relatively redundant, for example, lines 6, 14, 30, 40, 41, 42 all share this feature. Lines 1 and 3 are not vulnerable in the simulated typhoon, but switching them off can make output of generator 2 and 3 more reasonably distributed in the whole network.

3) However, the resilience enhancement effect of OTS weakens as contingency level and NSL increase. Under N-2 contingency, reduction of load-shedding weakens as NSL increases from 0 to 6, while under N-4, load-shedding remains the same as NSL increases from 3 to 9.

4) OTS shows more impact on reduction of WCEL than on NEL, for example, under N-3 contingency, with increasing of NSL, NEL keeps 3, while WCEL decreases from 9.22 MW to 6.86 MW. However, the impact of OTS on WCEL also weakens as contingency severity becomes worse.

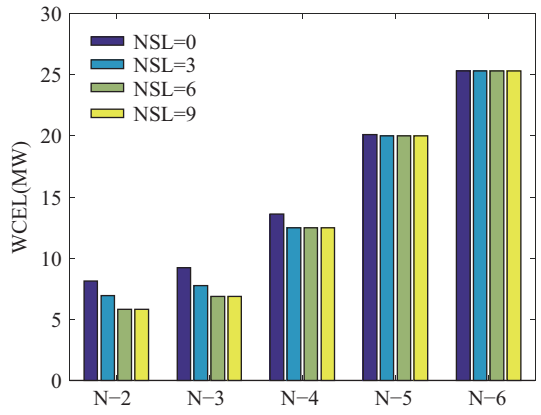

Fig. 6. WCEL results with different NSL and different contingency severity.

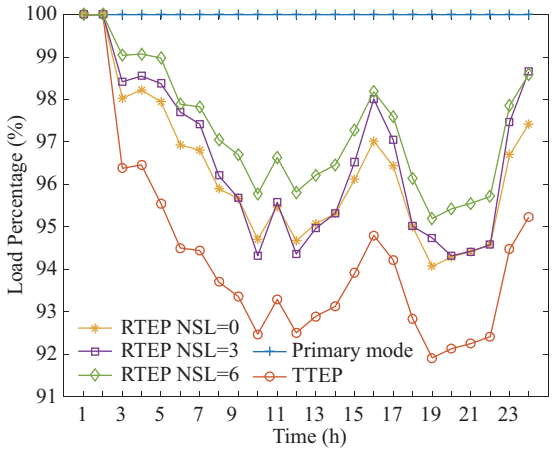

Fig. 7. The load percentage with different NSL and TEP model.

D. Impact of Vulnerability Uncertainty (VU)

The impact of VU is studied by setting VU to vary from

5% to 25%, that is, k_1 varies from 1.05∼1.25 while k_2 varies from 0.75∼0.95. As shown in Fig. 8 and 9, as VU increases from 5% to 25%, the NEL and WCEL keep increasing. However, the impact of VU varies with different contingency severity. In this case, the impact of UV under N-2 and N-4 is comparatively evident than under N-3, N-5∼N-6, where NEL remains the same when VU varies from 10%∼20%. Table IV shows results of RTEP with different VU under N-4. It can be seen that as VU increases from 5% to 25%, lines 15, 35, 37, 23, 39 are gradually added to the expansion plan to resist risk caused by higher failure rate uncertainty of transmission lines.

E. Impact of Cost of Load-shedding (CL)

The calculation of CL can be described as follows.

$$CL = CL_P * f_{ty} * 365 * 100 * 10^{-6} \tag{45}$$

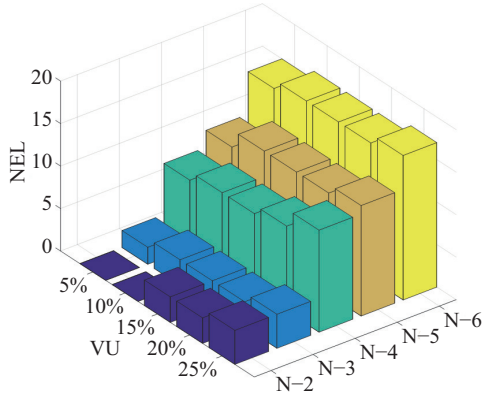

Fig. 8. NEL results with different VU and different contingency severity.

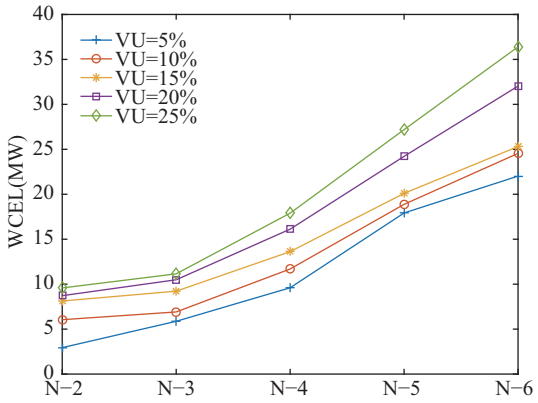

Fig. 9. WCEL results with different VU and different contingency severity.

TABLE IV
RESULTS OF RTEP WITH DIFFERENT VU UNDER N-4

VU	IC (M$)	LC (M$)	WCEL (MW)	EP	NEL
5%	8.49	0.96	9.60	9, 10, 18, 24, 25, 26, 29, 37	8
10%	9.49	1.17	11.69	9, 10, 15, 18, 24, 25, 26, 29, 37	9
15%	9.49	1.36	13.62	9, 10, 15, 18, 24, 25, 26, 29, 37	9
20%	10.6	1.61	16.12	9, 10, 15, 18, 24, 25, 26, 29, 35, 37	10
25%	12.73	1.79	17.90	9, 10, 15, 18, 23, 24, 25, 26, 29, 35, 37, 39	12

where CL_P is the cost of load-shedding, measured in $/MWh, f_{ty} is the frequency of typhoons in one year, 100 means 100 MVA, that is, the base value. (45) reveals the close association of frequency of typhoons, importance of load and CL. For example, $CL = 10$ may represent $f_{ty} = 20/365$ and $CL_P = 5000$, and $CL = 5$ may represent $f_{ty} = 10/365$ or $CL_P = 2500$, so that Cl reducing by half means the duration time of typhoon in a year or the importance of load in this area is reduced by half.

Table V and Fig. 10 and 11 show with increasing of CL, the NEL tends to slightly increase while the WCEL tends to be significantly reduced, showing the evident penalty effect of CL. For example, with contingency severity become worse, WCEL increases from 29.21 MW to 77.72 MW when $CL = 2.5$, and the WCEL only increase from 1.47 MW to 11.98 MW when $CL = 20$. However, impact of CL on RTEP weakens as

TABLE V
RESULTS OF RTEP WITH DIFFERENT CL UNDER N-4

CL (M$/p.u)	IC (M$)	LC (M$)	WCEL (MW)	EP	NEL
2.5	6.22	1.63	65.25	9, 10, 24, 26, 29, 37	6
5	8.35	1.22	24.37	9, 10, 15, 24, 25, 26, 29, 37	8
10	9.49	1.36	13.62	9, 10, 15, 18, 24, 25, 26, 29, 37	9
15	10.47	0.92	6.13	9, 10, 15, 18, 23, 24, 25, 26, 29, 37	10
20	10.47	1.23	6.13	9, 10, 15, 18, 23, 24, 25, 26, 29, 37	10

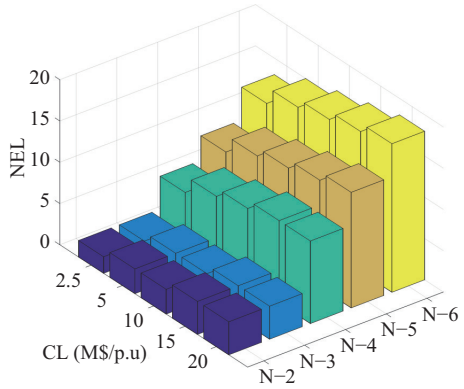

Fig. 10. NEL results with different CL and different contingency severity.

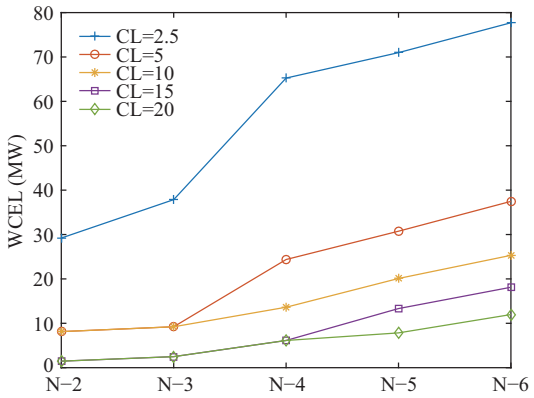

Fig. 11. WCEL results with different CL and different contingency severity.

CL increases from 15 to 20 because the increment of IC will be more than the decrement of LC, indicating that larger CL cannot lead to more investment in this case.

F. Computation Performance

Table VI shows the computation performance results. C3 represents the result of RTEP with OTS when NSL = 9. On one hand, more contingencies greatly increase computation time. From N-2∼N-6, computation time increases from 9 s to 4830 s in C1 although the iteration number only increases from 4 to 18. On the other, computation time and iteration number in C3 is more than in C1, indicating that binary OTS decision variables can evidently increase computation burden.

TABLE VI
COMPUTATION PERFORMANCE ON IEEE 30-BUS SYSTEM

C1	NEL	Iteration	Time (s)
N-2	3	4	9
N-3	3	4	23
N-4	9	11	376
N-5	12	15	1371
N-6	16	18	4830
C3	NEL	Iteration	Time (s)
N-2	2	4	25
N-3	3	7	145
N-4	8	15	898
N-5	12	22	3655
N-6	16	31	6632

G. Cases of 261-bus System of East China

The system consists of 261 buses, 156 generators, 326 existing lines and 326 candidate lines in the original corridor. Max load is 281,700 MW, the total generation capacity is 313,620 MW and the reserve ratio is 10.18%. The typhoon is simulated according to the same assumption as part A, and the track of typhoon is assumed to be within the area of 105,500 square kilometers where 68 transmission lines are located.

According to the typhoon model and component vulnerability curve, 56 lines in this area will be affected by the typhoon. We follow the same simulation procedure as previous part, and the results of RTEP without OTS (denoted as C4) and RTEP with OTS (denoted as C5) are presented in Table VII. It can be seen that more severe contingency leads to more transmission lines and WCEL. Moreover, OTS can reduce NEL from N-2∼N-6, indicating the effect of OTS is more significant for large-scale systems than small systems.

TABLE VII
RESULTS AND COMPUTATION PERFORMANCE OF 261-BUS SYSTEM

	C4			C5		
	NEL	WCEL (MW)	Time (h)	NEL	WCEL (MW)	Time (h)
N-2	17	10874	0.63	14	10025	1.07
N-3	24	14592	1.75	21	13614	3.76
N-4	33	20367	10.95	30	19186	12.84
N-5	38	24790	22.82	36	23947	25.97
N-6	45	31832	34.65	43	30941	40.95

VI. CONCLUSION

This paper proposes a RTEP with OTS model under typhoon weather. To model the component vulnerability uncertainty, a box uncertainty set characterizing the range of component failure rate under typhoon is constructed. TEP and OTS are modeled as long-term and short-term problems to balance resilience and economy of transmission network. Case studies reveal that: 1) based on the component vulnerability uncertainty model, the proposed RTEP method can better tradeoff resilience and economy cost compared with DAD model; 2) higher component vulnerability uncertainty tends to result in more transmission investments; 3) the effect of OTS is weakened as contingency caused by typhoon becomes worse, however, a larger network tends to be more flexible, thus the effect of OTS is more evident; 4) the algorithm developed can efficiently solve the proposed model even for a large-scale system. Promising future research may include: 1) combining TEP with more measures in different resilience phases, such as recovery measures, 2) integrate more long-term and short-term measures into TEP model, such as energy system, demand response, and so on.

REFERENCES

[1] X. Y. Jiang, J. Chen, M. Chen and Z. Wei, "Multi-stage dynamic post-disaster recovery strategy for distribution networks considering integrated energy and transportation networks," *CSEE Journal of Power and Energy Systems*, vol. 7, no. 2, pp. 408–420, Mar. 2021.

[2] X. R. Yang, L. Lü, L. X. Xu, Y. B. Liu, C. Z. Zhu, Q. Xiong, and Y. Li, "Probabilistic security evaluation of urban transmission considering elastic margin," *Power System Technology*, vol. 43, no. 2, pp. 705–713, Feb. 2019.

[3] M. Mahzarnia, M. P. Moghaddam, P. T. Baboli, and P. Siano, "A review of the measures to enhance power systems resilience," *IEEE Systems Journal*, vol. 14, no. 3, pp. 4059–4070, Sep. 2020.

[4] M. A. Mohamed, T. Chen, W. C. Su, and T. Jin, "Proactive resilience of power systems against natural disasters: A literature review," *IEEE Access*, vol. 7, pp. 163778–163795, Nov. 2019.

[5] X. Wang, Z. Y. Li, M. Shahidehpour, and C. W. Jiang, "Robust line hardening strategies for improving the resilience of distribution systems with variable renewable resources," *IEEE Transactions on Sustainable Energy*, vol. 10, no. 1, pp. 386–395, Jan. 2019.

[6] A. Bagheri, C. Y. Zhao, F. Qiu, and J. H. Wang, "Resilient transmission hardening planning in a high renewable penetration era," *IEEE Transactions on Power Systems*, vol. 34, no. 2, pp. 873–882, Mar. 2019.

[7] Y. X. Zhao, S. Y. Liu, Z. Z. Lin, L. Yang, Q. Gao, and Y. W. Chen, "Identification of critical lines for enhancing disaster resilience of power systems with renewables based on complex network theory," *IET Generation, Transmission & Distribution*, vol. 14, no. 20, pp. 4459–4467, Oct., 2020.

[8] H. Sabouhi, A. Doroudi, M. Fotuhi-Firuzabad, and M. Bashiri, "Electrical power system resilience assessment: A comprehensive approach," *IEEE Systems Journal*, vol. 14, no. 2, pp. 2643–2652, Jun. 2020.

[9] Y. P. Fang and G. Sansavini, "Optimizing power system investments and resilience against attacks," *Reliability Engineering & System Safety*, vol. 159, pp. 161–173, Mar, 2017.

[10] A. Bagheri and C. Y. Zhao, "Distributionally robust reliability assessment for transmission system hardening plan under $N-k$ security criterion," *IEEE Transactions on Reliability*, vol. 68, no. 2, pp. 653–662, Jun. 2019.

[11] S. S. Ma, B. K. Chen, and Z. Y. Wang, "Resilience enhancement strategy for distribution systems under extreme weather events," *IEEE Transactions on Smart Grid*, vol. 9, no. 2, pp. 1442–1451, Mar. 2018.

[12] W. Yuan, J. H. Wang, F. Qiu, C. Chen, C. Q. Kang, and B. Zeng, "Robust optimization-based resilient distribution network planning against natural disasters," *IEEE Transactions on Smart Grid*, vol. 7, no. 6, pp. 2817–2826, Nov. 2016.

[13] R. P. Liu, S. B. Lei, C. Y. Peng, W. Sun, and Y. H. Hou, "Data-based resilience enhancement strategies for electric-gas systems against sequential extreme weather events," *IEEE Transactions on Smart Grid*, vol. 11, no. 6, pp. 5383–5395, Nov. 2020.

[14] M. Shivaie, M. Kiani-Moghaddam, and P. D. Weinsier, "Resilience-based tri-level framework for simultaneous transmission and substation expansion planning considering extreme weather-related events," *IET Generation, Transmission & Distribution*, vol. 14, no. 16, pp. 3310–3321, Aug. 2020.
[15] H. Hamidpour, S. Pirouzi, S. Safaee, M. Norouzi, and M. Lehtonen, "Multi-objective resilient-constrained generation and transmission expansion planning against natural disasters," *International Journal of Electrical Power & Energy Systems*, vol. 132, pp. 107193, Nov. 2021.
[16] M. G. Firoozjaee and M. K. Sheikh-El-Eslami, "A hybrid resilient static power system expansion planning framework," *International Journal of Electrical Power & Energy Systems*, vol. 133, pp. 107234, Dec. 2021.
[17] J. H. Yan, B. Hu, K. G. Xie, J. J. Tang, and H. M. Tai, "Data-driven transmission defense planning against extreme weather events," *IEEE Transactions on Smart Grid*, vol. 11, no. 3, pp. 2257–2270, May 2020.
[18] B. Zhang, L. Zhang, W. Tang, Z. Wang and C. Wang, "A coordinated restoration method of electric buses and network reconfiguration in distribution systems under extreme events," *CSEE Journal of Power and Energy Systems*, doi: 10.17775/CSEEJPES.2020.04320.
[19] M. Panteli and P. Mancarella. "Influence of extreme weather and climate change on the resilience of power systems: Impacts and possible mitigation strategies," *Electric Power Systems Research*, vol. 127, pp. 259–270, Oct. 2015.
[20] B. Taheri, A. Safdarian, M. Moeini-Aghtaie, and M. Lehtonen, "Enhancing resilience level of power distribution systems using proactive operational actions," *IEEE Access*, vol. 7, pp. 137378–137389, Sep. 2019.
[21] M. Yan, X. M. Ai, M. Shahidehpour, Z. Y. Li, J. Y. Wen, S. Bahramira, and A. Paaso, "Enhancing the transmission grid resilience in ice storms by optimal coordination of power system schedule with pre-positioning and routing of mobile DC De-Icing devices," *IEEE Transactions on Power Systems*, vol. 34, no. 4, pp. 2663–2674, Jul. 2019.
[22] M. Panteli, D. N. Trakas, P. Mancarella, and N. D. Hatziargyriou, "Boosting the power grid resilience to extreme weather events using defensive islanding," *IEEE Transactions on Smart Grid*, vol. 7, no. 6, pp. 2913–2922, Nov. 2016.
[23] J. C. Liu, C. Qin, and Y. X. Yu, "Enhancing distribution system resilience with proactive islanding and RCS-based fast fault isolation and service restoration," *IEEE Transactions on Smart Grid*, vol. 11, no. 3, pp. 2381–2395, May 2020.
[24] C. Wang, P. Ju, S. B. Lei, Z. Y. Wang, F. Wu, and Y. H. Hou, "Markov decision process-based resilience enhancement for distribution systems: An approximate dynamic programming approach," *IEEE Transactions on Smart Grid*, vol. 11, no. 3, pp. 2498–2510, May 2020.
[25] M. H. Amirioun, F. Aminifar, and H. Lesani, "Resilience-oriented proactive management of microgrids against windstorms," *IEEE Transactions on Power Systems*, vol. 33, no. 4, pp. 4275–4284, Jul. 2018.
[26] M. H. Amirioun, F. Aminifar, and H. Lesani, "Towards proactive scheduling of microgrids against extreme floods," *IEEE Transactions on Smart Grid*, vol. 9, no. 4, pp. 3900–3902, Jul. 2018.
[27] C. Wang, Y. H. Hou, F. Qiu, S. B. Lei, and K. Liu, "Resilience enhancement with sequentially proactive operation strategies," *IEEE Transactions on Power Systems*, vol. 32, no. 4, pp. 2847–2857, Jul. 2017.
[28] S. Dehghan and N. Amjady, "Robust transmission and energy storage expansion planning in wind farm-integrated power systems considering transmission switching," *IEEE Transactions on Sustainable Energy*, vol. 7, no. 2, pp. 765–774, Apr. 2016.
[29] A. Khodaei, M. Shahidehpour, and S. Kamalinia, "Transmission switching in expansion planning," *IEEE Transactions on Power Systems*, vol. 25, no. 3, pp. 1722–1733, Aug. 2010.
[30] L. LiY. F. Mu, Z. L. Yin, H. J. Jia, X. H. Wang, G. L. Zhang, Identification method of weak links of overhead lines in distribution network based on typhoon scenario simulation," *Electric Power Automation Equipment*, vol. 05, no. 40, pp. 150–157, Apr. 2020.
[31] P. Zhang, G. F. Li, P. B. Luh, W. Y. Li, Z. H. Bie, and C. Serna, "Risk analysis for distribution systems in the Northeast U.S. under wind storms," in *Proceedings of the 2014 IEEE PES General Meeting | Conference & Exposition*, 2014, pp. 1.

Yang Yuan received the B.S. degree in Electrical Engineering from Wuhan University, China in 2016. He is currently working toward the Ph.D. degree with the Department of Electrical and Electronic Engineering, Shanghai Jiao Tong University. His research interests include resilience-oriented power system planning.

Heng Zhang received the Ph.D. degree in Electrical Engineering, Shanghai Jiao Tong University, Shanghai, China, in 2019. Now, he is an Assistant Researcher in Shanghai Jiao Tong University. His main research interests are power system planning and operation.

Haozhong Cheng received the Ph.D. degree in Power Systems from Shanghai Jiao Tong University, Shanghai, China, in 1998. He is currently a Professor in School of Electronic Information and Electrical Engineering, Shanghai Jiao Tong University. His research interests are mainly power system planning, operation, and deregulation.

Zheng Wang is a senior engineer of State Grid East China Branch. His research interests are mainly power system planning and operation.